

Lawrence Berkeley National Laboratory

Lawrence Berkeley National Laboratory

Title

Diluted magnetic semiconductors formed by an ion implantation and pulsed-laser melting

Permalink

<https://escholarship.org/uc/item/4sq318f8>

Authors

Scarpulla, M.A.

Daud, U.

Yu, K.M.

et al.

Publication Date

2003-07-23

Diluted magnetic semiconductors formed by ion implantation and pulsed-laser melting

M.A. Scarpulla^{1,2}, U. Daud^{1,2}, K.M. Yu², O. Monteiro², Z. Liliental-Weber², D. Zakharov²,
W. Walukiewicz², and O.D. Dubon^{1,2}

¹University of California at Berkeley, Berkeley, CA 94720, U.S.A.

²Lawrence Berkeley National Laboratory, Berkeley, CA 94720, U.S.A.

Using ion implantation followed by pulsed-laser melting (PLM), we have synthesized ferromagnetic films of $\text{Ga}_{1-x}\text{Mn}_x\text{As}$. Ion-channeling experiments reveal that these films are single crystalline and have high Mn substitutionality while variable temperature resistivity measurements reveal the strong Mn-hole interactions characteristic of carrier-mediated ferromagnetism in homogeneous DMS's. We have observed Curie temperatures (T_C 's) of approximately 80 K for films with *substitutional* Mn concentrations of $x=0.04$. The use of n-type counter doping as a means of increasing Mn substitutionality and T_C is explored by co-implantation of Mn and Te into GaAs. In $\text{Ga}_{1-x}\text{Mn}_x\text{P}$ samples synthesized using our technique, the implanted layer regrows as an epitaxial single crystal capped by a highly defective surface layer. These samples display ferromagnetism with $T_C \approx 23$ K.

Keywords:

GaMnAs, GaMnP, laser processing, ion implantation, diluted magnetic semiconductor

Corresponding Author:

M.A. Scarpulla; scarps@newton.berkeley.edu; Ph: (510) 486-5555; Fax: (510) 486-5530

Dept. of Materials Science & Engineering, 180 HMMB, UC Berkeley, Berkeley, CA 94720, USA

Diluted magnetic semiconductors (DMS's), especially ferromagnetic $\text{Ga}_{1-x}\text{Mn}_x\text{As}$, continue to be intensely investigated for applications in spin-based electronics [1,2]. $\text{Ga}_{1-x}\text{Mn}_x\text{As}$ exhibits ferromagnetism for $0.02 < x < 0.06$ with T_C 's exceeding 150 K after post-growth annealing [3-5]. Because the equilibrium solubility of transition metals is orders of magnitude lower than the concentrations required for ferromagnetism in III-V semiconductors, single-phase III-V DMS's are notoriously difficult to produce. Until now, low-temperature molecular beam epitaxy (LT-MBE) has been the only method proven capable of synthesizing epitaxial, single-phase III-V films. Attempts to produce $\text{Ga}_{1-x}\text{Mn}_x\text{As}$ using Mn ion implantation followed by conventional and rapid thermal annealing (RTA) have invariably led to the formation of (ferromagnetic) secondary phases [6-8]. Previous studies of Mn in GaP based on LT-MBE and on ion implantation followed by RTA have resulted in polycrystalline films [9-11].

Here we discuss the formation of III-V semiconductor films containing Mn using an alternative, versatile processing route: Mn ion implantation followed by pulsed-laser melting [12]. The rapid melting and recrystallization associated with PLM kinetically traps implanted species within regrown films at concentrations well in excess of equilibrium solubility limits whilst suppressing the formation of second phases [13].

Semi-insulating GaAs (001) wafers were implanted either with 80 keV Mn^+ ions or were implanted using the metal vapor vacuum arc (MEVVA) technique which we have described previously [12]. Each implanted sample was irradiated with a single pulse with fluence between $0.3 - 0.5 \text{ J/cm}^2$ from a KrF excimer laser ($\lambda = 248 \text{ nm}$, 38 ns FWHM) homogenized by a crossed cylindrical lens homogenizer. The structure of the layers and the location of Mn in the lattice were evaluated by 2 MeV $^4\text{He}^+$ channeling

Rutherford backscattering spectrometry (c-RBS) and particle induced X-ray emission (PIXE) along [001] and [011] directions [4]. A DC-SQUID magnetometer was used to measure the in-plane magnetic behavior of the films along a $\langle 100 \rangle$ direction. Temperature-dependent electrical resistivity was measured in the van der Pauw geometry using pressed In contacts.

Using c-RBS and PIXE, we find that the films are single-crystalline and that a large fraction of Mn is substitutional [12]. For example, the $\langle 110 \rangle$ minimum backscattered yield (χ_{\min}) is less than 0.046 for a film implanted with $5.2 \times 10^{15} / \text{cm}^2$ 80 keV Mn^+ and regrown with 0.36 J/cm^2 , which approaches the χ_{\min} of 0.027 for an as-received wafer. Roughly 65% of the Mn exists as Mn_{Ga} while the remaining fraction occupies non-commensurate locations, e.g. structural defects or the surface of the film. The Mn_{Ga} fraction typically decreases in our films with increasing Mn composition (to 40% for $x = 0.10$); however less than a few percent of the Mn in our films occupies interstitial sites. We attribute this absence of interstitials to annealing while the recrystallized film cools from its solidification temperature. This is in contrast to LT-MBE films where post-growth annealing is required to excise compensating interstitials [4].

The main panel of Fig. 1 presents the temperature variation of magnetization in an applied field of 50 Oe for a sample implanted with Mn to $7.5 \times 10^{15} / \text{cm}^2$ using MEVVA and irradiated at 0.3 J/cm^2 . The T_C of 64 K was determined by extrapolating the steep linear portion of the curve to zero. Inset a) depicts the peak in the temperature variation of sheet resistivity around T_C that is characteristic of carrier-mediated ferromagnetism in DMS's [14]. The variation of magnetization with magnetic field is presented in inset b)

and reveals a fairly square hysteresis loop which is similar to those observed in MBE-grown films [15] and is indicative of good crystal quality. Measurements between 2-5 T reveal that the moment per implanted Mn is *at least* $2.3 \mu_B$.

It has been observed in LT-MBE grown $\text{Ga}_{1-x}\text{Mn}_x\text{As}$ that the addition of Be causes substitutional Mn to move into interstitial sites. Based on these experiments, a model was proposed whereby the formation of compensating Mn interstitials is favored as the Fermi energy reaches a certain level with respect to the valence band, resulting in a saturation of the free-hole concentration around $10^{21} / \text{cm}^3$ [16]. Interstitial Mn are believed to be double donors and to couple antiferromagnetically to on-site Mn, hence they counter both the electronic and magnetic effects of substitutional Mn. [17]. Yu et al. have proposed that the T_C can be increased by counter doping films with saturated hole concentrations. The addition of compensating donors would increase the Mn_{Ga} concentration by suppressing the formation of Mn interstitials while maintaining the hole concentration at its saturation level [16].

We have investigated this hypothesis by counter doping with Te, for which substitutional incorporation in GaAs at atomic percent levels and with >90% substitutionality has been well demonstrated using ion implantation and PLM [18,19]. We note that a previous study found that adding Sn to $\text{Ga}_{1-x}\text{Mn}_x\text{As}$ decreased T_C with increasing amounts of Sn [20]. However, the Mn content in these films was well below the level required to saturate the hole concentration. Thus, counter doping reduced T_C by reducing the free-hole concentration below the saturation level.

We have prepared a series of films sequentially ion implanted with $2.08 \times 10^{16} / \text{cm}^2$ 80 keV Mn^+ and varying doses of 160 keV Te^+ and subsequently regrown using

PLM. For convenience in the following discussion, we define γ as the ratio of retained Te dose to retained Mn dose. Using the combination of c-RBS and PIXE we have determined that counter doping with Te does in fact increase the substitutionality of Mn. The substitutional Mn fraction in the film containing only Mn ($\gamma=0$) is approximately 40%, and this fraction increases to near 60% and to over 80% for $\gamma=0.33$ and 1, respectively. We note that only half of the implanted Mn dose is retained in the $\gamma=1$ sample due to sputtering.

Temperature dependent resistivity measurements of the Te counter doped films reveal that the $\gamma=0$ sample exhibits metallic conduction and a peak near its T_C of 77 K, which is a hallmark of critical scattering associated with hole-mediated ferromagnetism in metallic films [5]. The sample with $\gamma=0.33$ is p-type, is more resistive than the other films, and exhibits hopping conduction below ~ 25 K. Hall effect measurements revealed a reduced hole concentration, which indicates that the layer has been overcompensated. The sample with $\gamma \approx 1$ is n-type with a mean free-electron concentration of approximately $10^{18} / \text{cm}^3$.

Associated with the decrease in hole concentration and crossover to n-type conduction in the $\gamma > 0$ samples are dramatic changes in the magnetic behavior, as is seen in Fig. 2. The magnetization of the film containing Mn only has a shape typical of our $\text{Ga}_{1-x}\text{Mn}_x\text{As}$ films and exhibits a T_C of ~ 77 K. The n-type film with $\gamma \approx 1$ exhibits only paramagnetism. The intermediate film with $\gamma=0.33$ exhibits a rich temperature dependence involving a change in inflection and a long tail between 25 and 60 K. Magnetization versus applied field measurements on an identical sample reveal an open

hysteresis loop at 5 K and a Langevin-shaped magnetization curve with no hysteresis at 45 K.

We have also investigated the behavior of Mn in GaP as it has been suggested that $\text{Ga}_{1-x}\text{Mn}_x\text{P}$ may have a higher T_C than $\text{Ga}_{1-x}\text{Mn}_x\text{As}$. Fig. 3 presents a bright-field TEM cross-sectional image taken in a two-beam condition of a GaP film implanted with Mn to $7.5 \times 10^{15} / \text{cm}^2$ using MEVVA and regrown using PLM (0.4 J/cm^2). The presence of strain is indicated by the light and dark contrast. This image reveals that implantation and PLM results in single-crystal regrowth for $\sim 150 \text{ nm}$, but that a highly defective layer of $\sim 25 \text{ nm}$ is formed at the surface. No precipitates are apparent in the single crystalline region (region 2). SIMS measurements demonstrate the presence of Mn at concentrations up to 1.5 at% in the single crystalline region and channeling RBS and PIXE measurements indicate that 65% of this Mn is substitutional (i.e. x up to 0.02). The main panel of Fig. 4 presents the temperature variation of magnetization in a representative sample showing $T_C \sim 23 \text{ K}$. The inset of Fig. 4 presents the corresponding hysteresis loop obtained at 5 K. We are currently working to determine the origin of this ferromagnetism.

In conclusion, we have demonstrated the synthesis of ferromagnetic $\text{Ga}_{1-x}\text{Mn}_x\text{As}$ using ion-implantation followed by pulsed-laser melting. We show that the substitutional incorporation of Mn can be enhanced in $\text{Ga}_{1-x}\text{Mn}_x\text{As}$ by counter doping with Te. While the addition of Te at the levels described here led to a decrease in T_C (which, it should be possible to use implantation and PLM to tune the degree of compensation such that the concentration of substitutional Mn is increased maintaining a saturated hole concentration. It may also be possible to achieve large hole concentrations in such

material by spatially separating the compensated Mn containing material from heavily p-doped, e.g. by modulation doping or multilayer structures. Finally, we have investigated the regrowth of Mn ion implanted GaP and have found that single-crystalline regrowth with high Mn substitutionality is possible using our method.

This work was supported by the Director, Office of Science, Office of Basic Energy Sciences, Division of Materials Sciences and Engineering, of the U.S. Department of Energy under Contract No. DE-AC03-76SF00098. MAS acknowledges support from an NSF Graduate Research Fellowship. ODD acknowledges support from the Hellman Family Fund.

References

- [1] H. Ohno, *J. Cryst. Growth* 251 (2003) 285.
- [2] T. Dietl, arXiv: cond-mat/0306479 18 Jun 2003.
- [3] K.C. Ku et al., *Appl. Phys. Lett.* 82 (2003) 2302.
- [4] K.M. Yu et al., *Phys. Rev. B* 65 (2002) 201303.
- [5] T. Wojtowicz et al., *J. Supercond.* 16 (2003) 41.
- [6] J. Shi et al., *Nature* 377 (1995) 707.
- [7] P.J. Wellmann et al., *Appl. Phys. Lett.* 71 (1997) 2532.
- [8] J. Shi et al., *J. Appl. Phys.* 79 (1996) 5296.
- [9] N. Theodoropoulou et al., *Phys. Rev. Lett.* 89 (2002) 107203.
- [10] M.E. Overberg et al., *J. Vac. Sci. Technol., B* 20 (2002) 969.
- [11] M.E. Overberg et al., *Appl. Phys. Lett.* 79 (2001) 3128.
- [12] M.A. Scarpulla et al., *Appl. Phys. Lett.* 82 (2003) 1251.
- [13] M. Von Allmen and A. Blatter, *Laser-beam interactions with materials : physical principles and applications*. 2nd ed. Springer, New York, 1995, pp. 89-93.
- [14] T. Wojtowicz et al., submitted to *Appl. Phys. Lett.*
- [15] H. Ohno et al., *Appl. Phys. Lett.* 69 (1996) 363.
- [16] K.M. Yu et al., *Phys. Rev. B* 68 (2003) 041308(R).
- [17] J. Blinowski and P. Kacman, *Phys. Rev. B* 67 (2003) 121204(R).
- [18] P.A. Barnes et al., *Appl. Phys. Lett.* 33 (1978) 965.
- [19] J.M. Poate and J.W. Mayer, *Laser annealing of semiconductors*. Academic Press, New York, 1982.
- [20] Y. Satoh et al., *Physica E*, 10 (2001) 196.

Figure Captions

Fig. 1 – (Main] Temperature variation of magnetization with an applied field of 50 Oe for a $\text{Ga}_{1-x}\text{Mn}_x\text{As}$ sample produced using our technique. The T_C of 64 K is indicated by the arrow. (Inset a) Temperature variation of sheet resistivity for an identical sample. The arrow points out the peak near T_C that is a hallmark of carrier-mediated ferromagnetism. (Inset b) Magnetization vs. applied field at 5 K for the sample depicted in the main panel.

Fig. 2 – Temperature variation of the magnetization for the samples the Te counter doped $\text{Ga}_{1-x}\text{Mn}_x\text{As}$ samples.

Fig. 3 – Cross-sectional bright field TEM image of a Mn ion implanted and PLM regrown GaP film taken in a two-beam condition ($g = 200$). The damaged surface layer is designated as region 1, the regrown film is designated as region 2, while the GaP substrate is designated as region 3. The contrast in this image is indicative of the presence of strain and dislocations.

Fig. 4 – (main) Temperature variation of magnetization for a $\text{Ga}_{1-x}\text{Mn}_x\text{P}$ sample. The arrow indicates the T_C of 23 K. (Inset) Magnetization vs. applied field at 5 K for the sample depicted in the main panel.

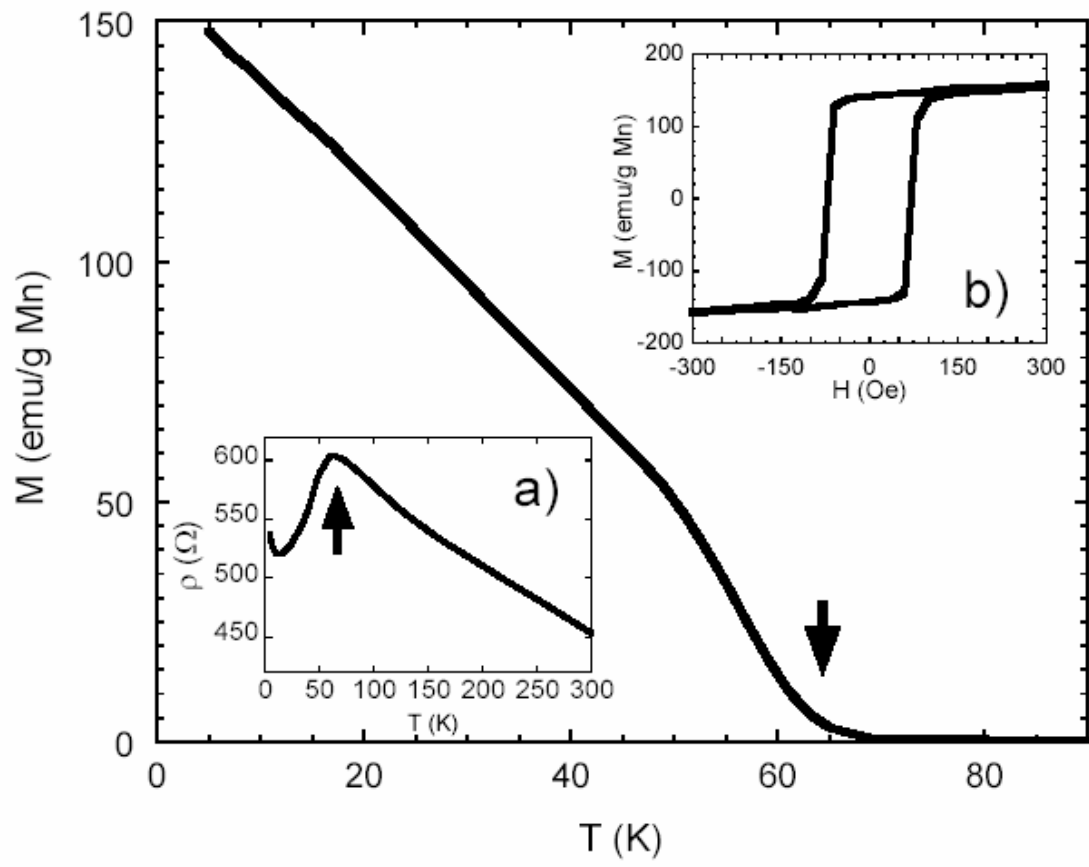


Figure 1 - M.A. Scarpulla et al.

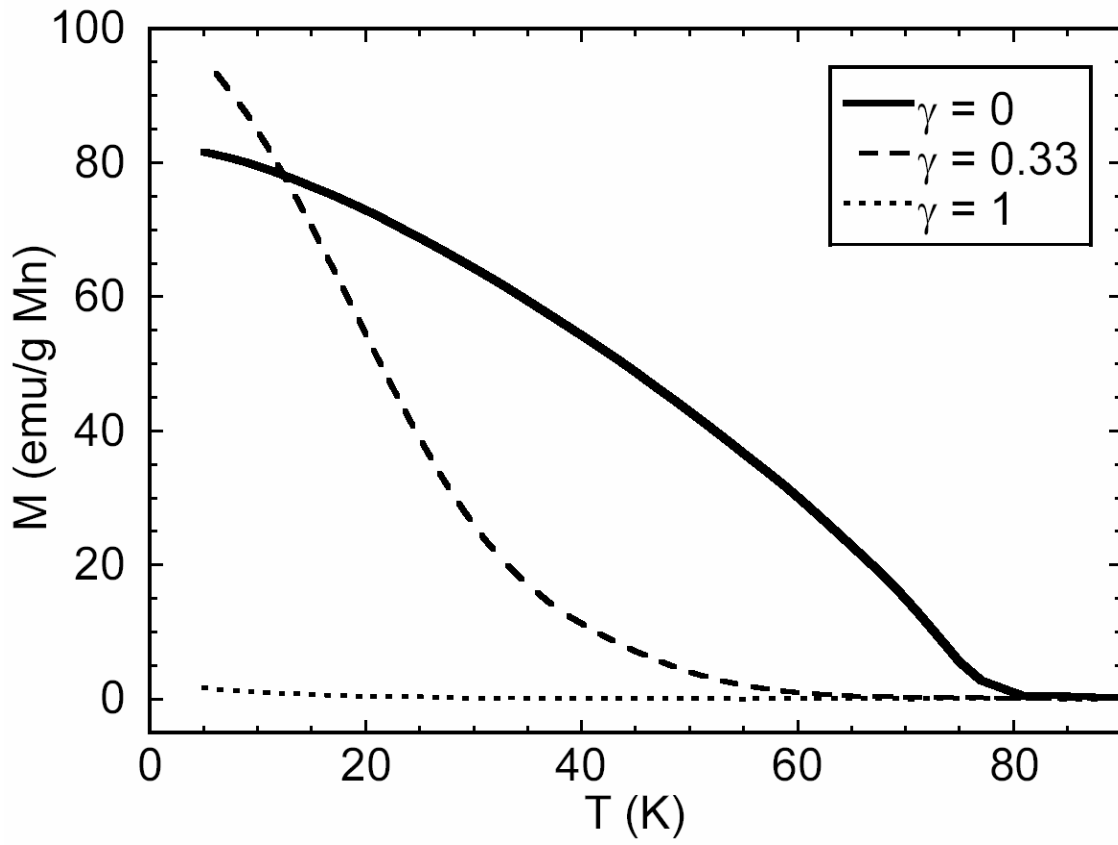


Figure 2 - M.A. Scarpulla et al.

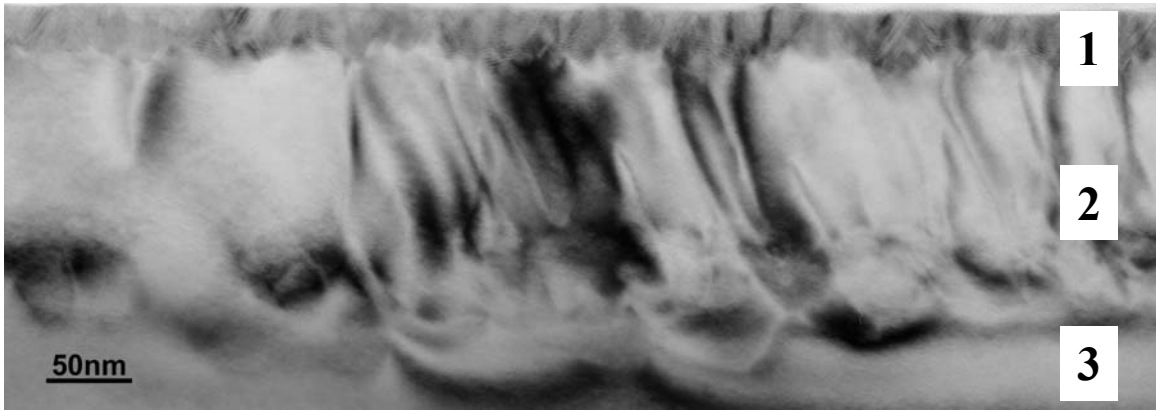


Figure 3 - M.A. Scarpulla et al.

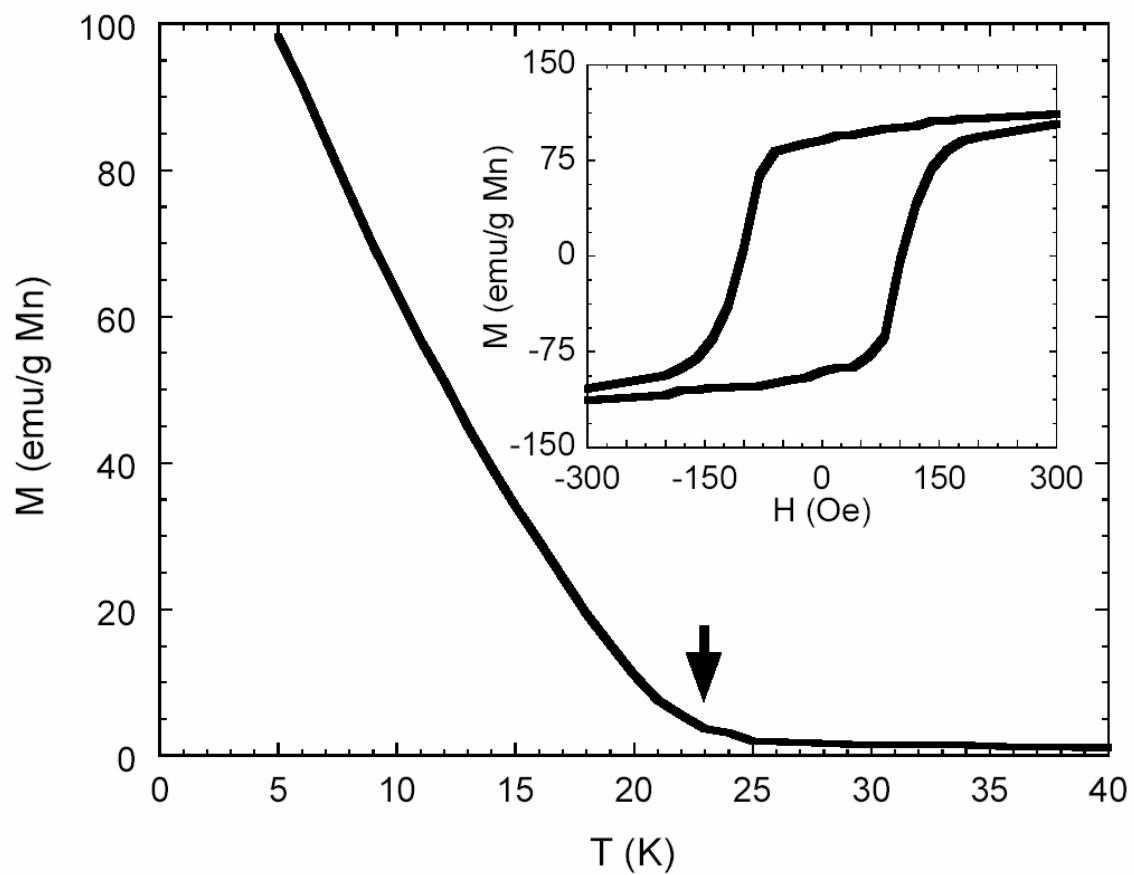


Figure 4 - M.A. Scarpulla et al.